Title	Analysis and stabilization of chaos in electric-vehicle steering system
Author(s)	ZHANG, Z; Chau, KT; Wang, Z
Citation	IEEE Transactions on Vehicular Technology, 2013, v. 62 n. 1, p. pp. 118-126
Issued Date	2013
URL	http://hdl.handle.net/10722/189041
Rights	Creative Commons: Attribution 3.0 Hong Kong License

Analysis and Stabilization of Chaos in the Electric-Vehicle Steering System

Zhen Zhang, K. T. Chau, *Senior Member, IEEE*, and Zheng Wang, *Member, IEEE*

***Abstract*—This paper presents a new control method to improve the safety performance of the electric-vehicle (EV) steering system. It is found that the EV steering system exhibits unstable chaotic behaviors at certain speeds, which can deteriorate the steering performance and even make vehicles fall into spin. In this paper, a new dynamic model is proposed to describe the EV steering system, which takes into account the motor drive for EV propulsion. Moreover, both the driver's reaction time and the disturbance caused by irregularities of the road surface are also incorporated into the EV steering model. It can be identified that periodic, quasi-periodic, and chaotic motions occur at the EV steering system with respect to different forward speeds. Thus, a new control scheme, namely the adaptive time-delayed feedback control (ATDFC), is proposed and implemented to stabilize the EV steering system from chaos to stable operation. Finally, the validity of the proposed model and control are verified.**

***Index Terms*—Adaptive time-delayed feedback control (ATDFC), chaos, electric vehicle (EV), stabilization, steering system.**

I. Introduction

WITH EVER growing consumption of traditional forms of energy, the study of electric vehicles (EVs) has attracted considerable attention [1], [2]. Since the traditional engine is replaced by the electric motor, the concept of zero local emission is truly realized in EVs. The problem of environmental pollution can thus be alleviated. Along with the development of EVs, safety performance has become a major concern for many researchers. According to various studies on the causes of traffic accidents, the stability of the vehicle steering system is an important issue. Unstable dynamic lateral behaviors may cause vehicles to go out of control and even fall into a spin. While EVs are commercialized and becoming more and more popular, the stability and maneuverability of the EV steering system should be improved under various driving conditions, with a particular focus on the safety of critical cornering behaviors in an emergency.

For the steering system, studies on the safety of vehicles, particularly at a high forward speed, have received considerable attention from both the automotive industry and research institutions. A number of ideas related to steering control have been tested in experimental prototypes. As early as 1969, Kasselmann and Keranen proposed an active steering system based on a feedback signal from a yaw-rate sensor [3]. In 1976, Fenton *et al.* also proposed the theory of the steering system and tested several controller designs by experiments [4]. Along with the development of nonlinear dynamics, particularly the chaos theory and its corresponding analytical techniques [5]–[7], complex nonlinear characteristics were revealed in the vehicle steering system [8], [9]. As a result, many linear and nonlinear control methods were successfully designed and implemented for the steering system. For example, a linear controller and a nonlinear controller based on the feedback of the lateral displacement and the yaw rate were proposed in [10] and [11]. In 2007, Cai *et al.* developed a genetic fuzzy controller for automatic steering of a small-scale vehicle [12]. An adaptive steering system, which consists of a vehicle directional control unit and a driver interaction unit, was designed and implemented by Cetin *et al.* [13]. Additionally, a steering system with a new mechanical structure, namely the steer-by-wire system, was also presented in [14] and [15].

However, the aforementioned studies only focus on improving the mechanical structure or the control algorithm for the steering system. The driver's reaction time is seldom considered in the dynamic analysis. In addition, the external perturbation is ignored by many researchers, which can actually cause instability of the steering system. Such external perturbation includes the disturbance caused by irregularities of the road surface, backlashes caused by the driving gear, and wind gust. In addition, most research is targeted at the steering system for traditional vehicles and not for EVs. For example, the electric motor that is used for EV propulsion has complex nonlinear dynamic behaviors. Thus, the dynamic behaviors of the EV steering system cannot be properly described if the effect of the electric motor is ignored.

The purpose of this paper is to analyze the chaotic behavior of the EV steering system, and then propose a control scheme to stabilize the system from chaos to stable operation. The key is to take into account the characteristics of the electric motor for EV propulsion. In addition, the human reaction time and the disturbance caused by irregularities of the road surface are considered in the mathematical model of the EV steering system.

This paper is mainly comprised of four parts: mathematical modeling, nonlinear analysis, a control strategy, and verification results. In Section II, a new mathematical model of the EV steering system will be proposed, where the electric motor characteristics, driver's reaction time, and disturbance caused by irregularities of the road surface are taken into account.

Manuscript received March 12, 2012; revised July 8, 2012; accepted August 31, 2012. Date of publication September 7, 2012; date of current version January 14, 2013. This work was supported in part by the Hong Kong Research Grants Council under Project HKU710710E. The review of this paper was coordinated by Prof. T. M. Guerra.

Z. Zhang and K. T. Chau are with the Department of Electrical and Electronic Engineering, The University of Hong Kong, Pokfulam, Hong Kong (e-mail: ktchau@eee.hku.hk).

Z. Wang is with the School of Electrical Engineering, Southeast University, Nanjing 210096, China.

Color versions of one or more of the figures in this paper are available online at http://ieeexplore.ieee.org.

Digital Object Identifier 10.1109/TVT.2012.2217767

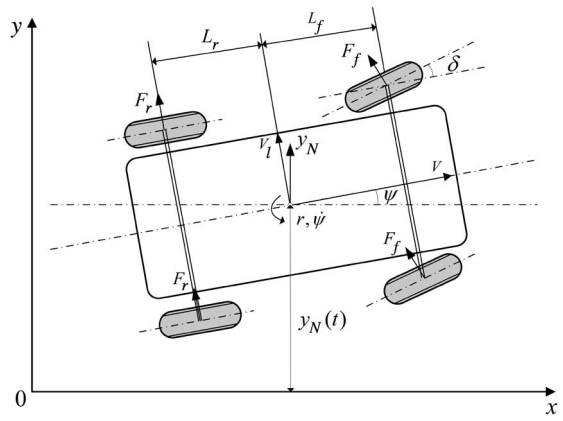

Fig. 1. EV lateral model in a fixed coordinate system.

At this stage, the permanent-magnet dc (PMDC) motor will be used for exemplification, which is valid for those low-cost EVs. In Section III, based on the proposed model, various nonlinear analysis methods will be utilized to investigate the chaotic behavior of the EV steering system when the forward speed exceeds the threshold. Then, in Section IV, a new control algorithm based on the adaptive time-delayed feedback control (TDFC) method will be proposed and implemented to stabilize the chaotic behavior of the EV steering system. Since the control method is considered a general approach to stabilizing a class of continuous-time chaotic systems with a time delay, the discussion will be focused on its implementation for the proposed EV steering model, whereas its mathematical derivation will be delineated in a general form in the Appendix. Consequently, in Section V, detailed simulation results will be provided to verify the validity of the proposed model and the control method.

II. Modeling

Unlike traditional vehicles, EVs are propelled by electric motors. Thus, the dynamic characteristics of the electric motor significantly affect the EV steering system. Here, a new mathematical model specifically describing the EV steering system is developed, where the model of the steering system and the model of the electric motor are newly incorporated together for nonlinear analysis and controller design. Additionally, both the driver's response and the disturbance resulting from irregularities of the road surface are considered in this modeling.

For modeling, the EV has a rigid mass and a constant forward speed along a straight road. The center of gravity of the EV is located in a body-fixed local coordinate system, as shown in Fig. 1. Thus, the EV steering motions can be described by 2-D differential equations.

First, the equation of lateral motion is given by

$$m(\dot{V}_l + V_y V) = 2F_f \cos\delta + 2F_r \tag{1}$$

where V_l is the lateral velocity in the local coordinate system, V_y is the yaw velocity with respect to the local coordinate system, V is the EV forward speed, F_f and F_r, respectively, represent the front and rear wheel lateral forces resulting from the friction between the tires and the road surface, m is the mass of the EV, and δ is the resulting steering angle applied on the front wheels.

TABLE I
Coefficients of Tire Models

Road surface	Wheel	B_f, B_r	C_f, C_r	D_f, D_r	E_f, E_r
High-friction road	Front	6.7651	1.3000	-6436.8	-1.9990
	Rear	9.0051	1.3000	-5430.0	-1.7908
Low-friction road	Front	11.275	1.5600	-2574.7	-1.9990
	Rear	18.631	1.5600	-1749.7	-1.7908

Second, the equation of yaw motion is given by

$$I_z \dot{\gamma} = 2L_f F_f \cos\delta - 2L_r F_r \tag{2}$$

where L_f is the distance from the front axle to the center of gravity, L_r is the distance from the rear axle to the center of gravity, and I_z is the yaw moment of inertia of the EV body about the vertical axis.

In this model, consisting of (1) and (2), F_f and F_r are functions of the physical properties of the tires and of the sideslip angles (α_f, α_r) on the front and rear wheels, respectively. Thus, the EV dynamic behaviors depend on the accuracy of the tire model. Accordingly, many researchers have proposed various tire models, particularly on how to describe its cornering force characteristics. Among them, a mathematical model called the magic formula [16] is identified to be the most viable and practical for implementation, which is given by

$$F_f = D_f \sin\left\{C_f \tan^{-1}\left[B_f(1-E_f)\alpha_f + E_f \tan^{-1}(B_f\alpha_f)\right]\right\} \tag{3}$$

$$F_r = D_r \sin\left\{C_r \tan^{-1}\left[B_r(1-E_r)\alpha_r + E_r \tan^{-1}(B_r\alpha_r)\right]\right\} \tag{4}$$

where the numerical coefficients B_i, C_i, D_i, and $E_i (i = f, r)$ are listed in Table I.

In the fixed coordinate system, as shown in Fig. 1, (x_N, y_N) denotes the coordinate of the center of mass G, and ψ represents the EV heading angle with respect to the road center line. Then, it yields

$$\dot{y}_N = V_l \cos\psi + V \sin\psi \tag{5}$$

$$\dot{\psi} = V_y. \tag{6}$$

Equation (5) can be written as

$$V_l = \frac{(\dot{y}_N - V\sin\psi)}{\cos\psi}. \tag{7}$$

Equations (1) and (2) can be written as

$$\dot{V}_l = \frac{2F_f \cos\delta + 2F_r}{m} - V_y V \tag{8}$$

$$\dot{V}_y = \frac{2L_f F_f \cos\delta - 2L_r F_r}{I_z}. \tag{9}$$

By differentiating (8) and (9) with respect to time t and substituting (5) and (6), the basic model describing the lateral dynamics of the EV in the fixed coordinates can be obtained as

$$\ddot{y}_N = \frac{2[F_f \cos\delta + F_r]\cos\psi}{m} - \tan\psi[\dot{y}_N - V\sin\psi]\dot{\psi} \quad (10)$$

$$\ddot{\psi} = \frac{2[L_f F_f \cos\delta - L_r F_r]}{I_z}. \quad (11)$$

For EV propulsion, different types of electric motors can be used [1]. For simplicity, the PMDC motor is adopted for exemplification. It should be noted that when the ac motor is adopted, the use of vector control can transform the control variables to dc quantities similar to that of dc motors. The mathematical model of the PMDC motor [1] can be expressed as

$$\dot{\omega} = \frac{K_T I_a - B_m\omega - T_l}{J_m} \quad (12)$$

$$\dot{I}_a = \frac{V_{\text{in}} - K_E\omega - R_a I_a}{L_a} \quad (13)$$

where ω is the motor rotational speed, I_a is the armature current, K_T is the torque constant, K_E is the back electromotive force constant, R_a is the armature resistance, L_a is the armature inductance, B_m is the viscous damping, J_m is the moment of inertia, T_l is the restoring torque, and V_{in} is the input voltage.

Additionally, the relation between V and ω can be expressed as

$$V = n\omega R \quad (14)$$

where R represents the radius of the tire and n is the speed reduction ratio between the motor rotational speed and the vehicle forward speed. By substituting (14) to (10), it yields

$$\ddot{y}_N = \frac{2[F_f\cos\delta + F_r]\cos\psi}{m} - \tan\psi[\dot{y}_N - n\omega R\sin\psi]\dot{\psi}. \quad (15)$$

Therefore, the mathematical model of the EV steering system in the fixed coordinate system can be described by (11)–(13), and (15).

In this paper, the time delay impact on the stability of the EV steering system, which is caused by the driver's response, is considered. The driver's model proposed in [17] is adopted as follows:

$$\delta(t) = -K\left[y(t-T_r) + \frac{L}{V}\dot{y}(t-T_r)\right] \quad (16)$$

where $\delta(t)$ denotes the steering angle from the driver's response, and T_r denotes the time delay caused by the driver's response.

Additionally, vehicles are readily affected by external disturbances, such as irregularities of the road surface, backlashes from the driving gear, wind gusts, etc. Thus, the disturbance term $Q\cos(2\pi f_d t)$ is included to take into account the possible external disturbances occurring in the EV steering system, where Q denotes the amplitude of the periodic disturbance [18]. Hence, the resulting steering angle $\delta(t)$ can be expressed as

$$\delta(t) = -K\left[y(t-T_r) + \frac{L}{n\omega R}\dot{y}(t-T_r)\right] + Q\cos(2\pi f_d t) \quad (17)$$

where the disturbance frequency f_d is related to the EV forward speed V and a constant disturbance gain K_d. It is given by

$$f_d = K_d V. \quad (18)$$

Therefore, the EV steering system equations can be written in state form as follows:

$$\dot{x}_1 = x_3 \quad (19)$$

$$\dot{x}_2 = x_4 \quad (20)$$

$$\dot{x}_3 = \frac{2[F_f\cos\delta(t) + F_r]\cos x_2}{m} - \tan x_2[x_3 - n\omega R\sin x_2]x_2 \quad (21)$$

$$\dot{x}_4 = \frac{2[L_f\cos\delta(t) - L_r F_r]}{I_z} \quad (22)$$

$$\dot{x}_5 = \frac{K_T x_6 - B_m x_5 - T_l}{J_m} \quad (23)$$

$$\dot{x}_6 = \frac{V_{\text{in}} - K_E x_5 - R_a x_6}{L_a} \quad (24)$$

where $x(t) = (y_N, \psi, \dot{y}_N, \dot{\psi}, \omega, I_a)$.

Thus, the sideslip angles of front and rear wheels in terms of the state variables are, respectively, obtained as

$$\alpha_f = \arctan\left[\frac{x_3 - nx_5 R\sin x_2 + L_f x_4\cos x_2}{V\cos x_2}\right] - \delta(t) \quad (25)$$

$$\alpha_r = \arctan\left[\frac{x_3 - nx_5 R\sin x_2 - L_r x_4\cos x_2}{V\cos x_2}\right]. \quad (26)$$

Finally, the aforementioned modeling is based on some assumptions or working hypotheses that are evaluated as follows.

1) With respect to the EV weight, the human's weight takes only a small proportion. Thus, it is ignored in the proposed EV steering model. Since the mass is independent of time, the mass discrepancy caused by this assumption will not significantly affect the dynamic characteristics of the EV steering system.
2) The time delay caused by the steering mechanism is ignored since it is far less than the delay resulting from human response. Thus, the driver's response time is considered as the only time delay existing in the proposed EV steering model.
3) The rolling resistance of vehicle tires theoretically depends on the tire types, tire pressure, tire temperature, vehicle speed, tread thickness, number of plies, and torque transmitted level. Since its variation is not so significant as compared with the road load, it is assumed to be a constant and absorbed into the restoring torque.
4) In reality, the disturbance caused by the irregularity of the road is very complex. To investigate the robustness of the proposed control method, the corresponding disturbance is assumed to be $Q\cos(2\pi f_d t)$, as proposed in [18].

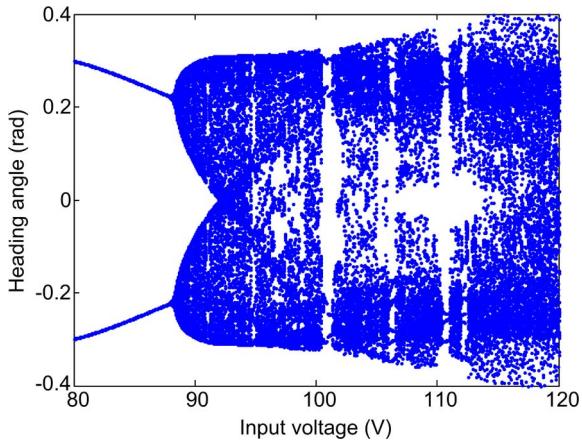

Fig. 2. Bifurcation diagram.

III. Analysis

To assess the safety of the EV steering system, the nonlinear dynamics of the ψ are studied with respect to different V's. Since the $V_{\rm in}$ is generally used to perform speed control of the PMDC motor, the relationship between the ψ and the $V_{\rm in}$ is analyzed.

Nonlinear characteristics of the EV steering system can be observed by the bifurcation diagram, the largest Lyapunov exponent, phase portraits, or power spectra. In this paper, numerical simulations of the EV steering system described by (19)–(24) are carried out by using the Runge–Kutta method. Parameters of the EV steering system and the driver's response model are $n=1.3$, $m=740$ kg, $I_z=2900$ kg $\cdot$ m^2, $L_f=1.1$ m, $L_r=1.4$ m, $R=0.3$ m, $K=0.009$ rad/m, $L=65$ m, $K_d=0.022$, $Q=0.05$ rad, $T_r=0.2$ s, $K_T=0.584$ (N $\cdot$ m)/A, $K_E=0.584$ V/rad/s, $J_m=0.08$ kg $\cdot$ m^2, $B_m=0.015$ (N $\cdot$ m)/rad/s, $R_a=0.1\ \Omega$, $L_a=0.008$ H, and $T_l=7$ N $\cdot$ m.

The bifurcation diagram is a widely used technique to describe the transition from periodic motion to chaotic motion for a dynamic system. Fig. 2 shows the bifurcation diagram of the ψ with respect to $V_{\rm in}$. It shows that the heading angle stays in the state of stable periodic oscillation for $V_{\rm in} < 88$ V, namely the EV forward speed is less than 15 m/s. When $V_{\rm in}$ is increased to 88 V, the system dynamics start to bifurcate so that the dynamic behavior varies qualitatively, namely the EV steering system exhibits quasi-periodic and then chaotic oscillations. With further increasing $V_{\rm in}$, the amplitude of chaotic oscillations tends to grow larger. Meanwhile, the heading angle intermittently transits to periodic oscillations and then back to the chaotic state. In addition, the corresponding time responses, phase portraits, and power spectra can also illustrate its route to chaos.

Fig. 3 describes the time response of the ψ with respect to the $V_{\rm in}$. As shown in Fig. 3(a), it can be seen that the ψ oscillates with a constant period when the $V_{\rm in}$ is equal to 82 V. Along with the increasing bifurcation parameter, the ψ exhibits the stable period-2 orbits, as shown in Fig. 3(b). Fig. 3(c) shows that the EV steering system enters into the chaotic domain. By choosing the $V_{\rm in}$ as 110.8 V, Fig. 3(d) shows that the system escapes from the chaos back to the period-3 oscillation. When the voltage increases beyond 111 V, the chaos in the EV heading angle ψ occurs again.

The phase portrait with the heading angle versus its velocity is provided in Fig. 4. It also indicates a transition of the dynamic behaviors from periodic, quasi-periodic, and chaotic motions. It can be seen that periodic-n motion occurs when the $V_{\rm in}$ equals 82 V, 101.2 V, and 110.8 V, as shown in Fig. 4(a), (b), and (d), whereas the chaotic oscillation can be observed when $V_{\rm in}$ is 107 V, as shown in Fig. 4(c).

Additionally, the Lyapunov exponents can qualify the rates of stretching and squeezing of the attractor in the state space, and indicate the exponential rate of the divergence and convergence of close trajectories. Thus, the largest Lyapunov exponent $\lambda_{\max}$ is calculated to mathematically verify the existence of chaos. The solution flow of the system state variables is expressed as

$$X(t) = T^t X_0 \tag{27}$$

where Tt is the map describing the time-t evolution of X, and the solution flow of their deviation δX is given by

$$\delta X(t) = U^t_{X_0} \delta X_0 \tag{28}$$

where $U^t_{X_0}$ is the map describing the time-t evolution of δX. By taking the evolution time $\Delta t \ll 1$ and the ith orthogonal and normal base vector of the d-dimension state space at the jth step $\|e^j_i \ll 1\|$, the Lyapunov exponent λ_i $(i = 1 \sim d)$ of the d-dimension system can be obtained as [19]

$$\lambda_i = \lim_{h\to\infty} \frac{1}{h\Delta t} \sum_{j=0}^{h-1} \log \frac{\left\| T^{\Delta t}\left(X_j + e^j_i\right) - T^{\Delta t}(X_j) \right\|}{\left\| e^j_i \right\|}. \tag{29}$$

Since the proposed dynamic system has a time-delayed component, the state variable on the interval $[t, t-\tau]$ can be approximated by N samples taken at intervals $\Delta t = \tau/(N-1)$. Therefore, the largest Lyapunov exponent can be computed [20]. To mathematically verify the results in Figs. 5–7, the largest Lyapunov exponents are calculated. By using MATLAB, the largest Lyapunov exponents are -1.011, -0.875, and -0.648, when $V_{\rm in}$ is equal to 82, 101.2, and 110.8 V, respectively. These negative values mean that the flow solutions attract to a stable fixed point or a stable periodic orbit. When the voltage $V_{\rm in}$ is set as 107 V, the largest Lyapunov exponent becomes positive, which is 1.215. This indicates that the solution of the dynamic system displays chaotic oscillation.

IV. Adaptive Time-Delayed Feedback Control

The TDFC method is one of the most appealing methods to suppress chaos [21]. The key of the TDFC method is to add a proportional variable to the difference of the state variables between the current state and the one-period delayed state. It has been successfully used in industry applications. Nevertheless, the effectiveness of the TDFC method is easily affected by the system parameter variations.

Consequently, this paper presents a modified TDFC by using an adaptive law to tune the feedback gain. The new control scheme, namely the adaptive TDFC (ATDFC), can drive the EV steering system from chaos to stable periodic behaviors effectively. In addition, it remains insensitive to the system parameter variations while it improves the robustness of the controlled system.

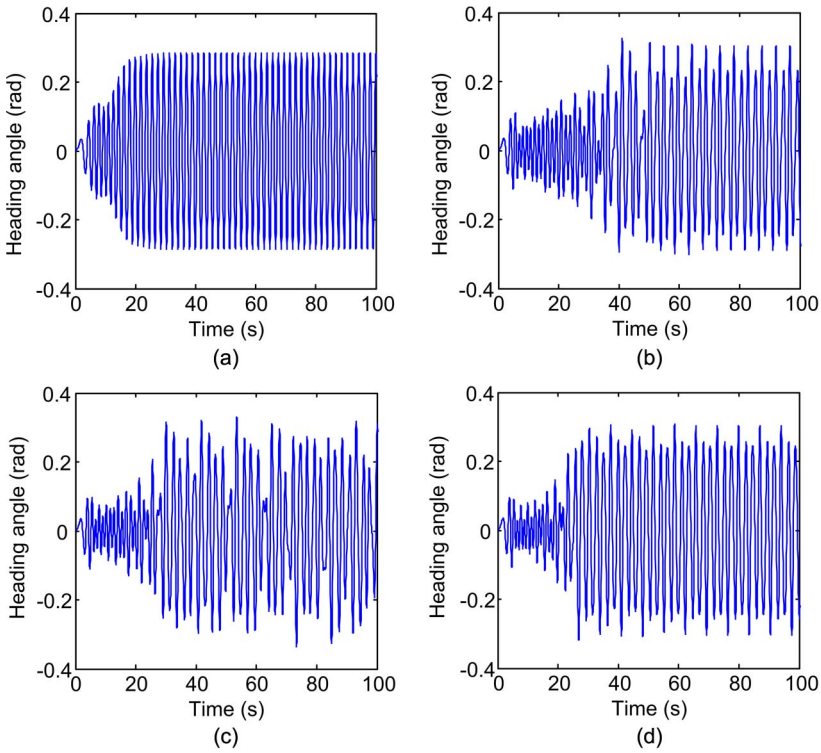

Fig. 3. Time responses of EV heading angle ψ. (a) $V_{\rm in} = 82$ V. (b) $V_{\rm in} = 101.2$ V. (c) $V_{\rm in} = 107$ V. (d) $V_{\rm in} = 110.8$ V.

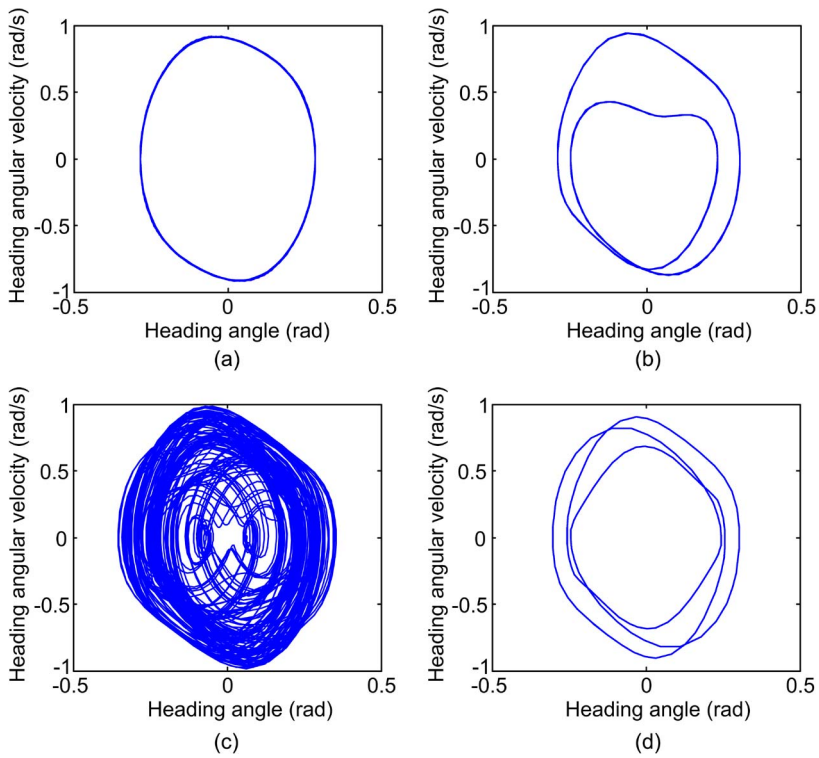

Fig. 4. Phase portraits of EV heading angle ψ versus the velocity $\psi^{(1)}$. (a) $V_{\rm in} = 82$ V. (b) $V_{\rm in} = 101.2$ V. (c) $V_{\rm in} = 107$ V. (d) $V_{\rm in} = 110.8$ V.

First, the steering system is expressed in a linear form by using Talyor expansion. Second, based on the linearized model, the proposed ATDFC law is incorporated as given by (31), where the corresponding adaptive gain matrix is governed by (32). In the controller model, the control matrix B, the positive definite matrix P, and the gain η are chosen in such a way that the control performance is acceptable. Third, the controller time delay is optimally chosen according to the gradient-descent approach [22]. It should be noted that the mathematical proof of the proposed ATDFC method in a closed loop for a general class of continuous-time chaotic systems with time delay is shown in the Appendix.

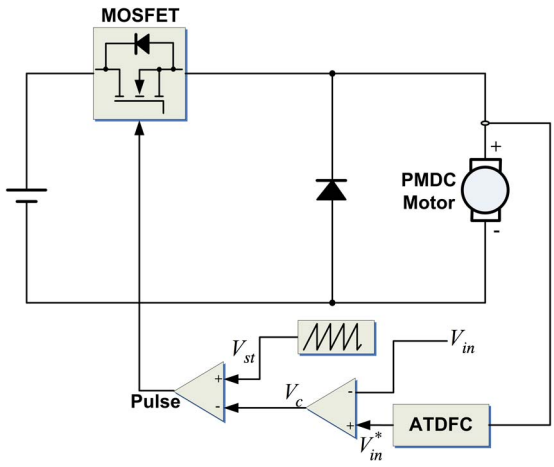

Fig. 5. PWM dc-dc converter with ATDFC.

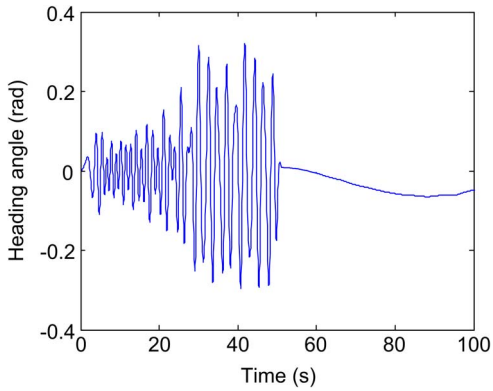

Fig. 6. Time response of heading angle ψ using the ATDFC method ($V_{\text{in}} = 107$ V).

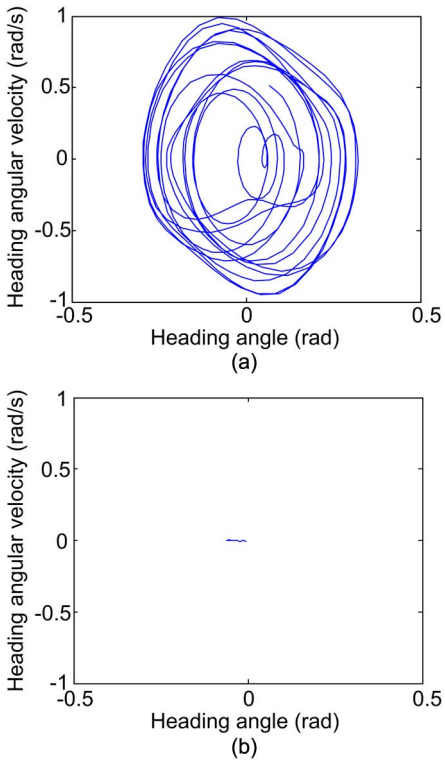

Fig. 7. Phase portrait of heading angle ψ versus the velocity $\psi^{(1)}$ ($V_{\text{in}} = 107$ V). (a) When $t \in [0, 50]$. (b) When $t \in (50, 100]$.

To design the controller, the EV steering system is first represented by

$$\dot{x}(t) = Ax(t) + A'x(t - T_r) \tag{30}$$

where A and A' are the Jacobian matrices of the nonlinear function f with respect to $x(t)$ and to $x(t - T_r)$, respectively, as given by

$$A = \frac{\partial f}{\partial x(t)} \quad \text{and} \quad A' = \frac{\partial f}{\partial x(t - T_r)}.$$

By using MATLAB, it yields

$$A = \begin{bmatrix} 0 & 0 & 1 & 0 & 0 & 0 \\ 0 & 0 & 0 & 1 & 0 & 0 \\ 0 & A_{32} & A_{33} & A_{34} & 0 & 0 \\ 0 & A_{42} & A_{43} & A_{44} & 0 & 0 \\ 0 & 0 & 0 & 0 & A_{55} & A_{56} \\ 0 & 0 & 0 & 0 & A_{65} & A_{66} \end{bmatrix}$$

where $A_{32} = 4BCD/m$, $A_{33} = -4BCD/mRn$, $A_{34} = -2BCD(L_f - L_r)/mRn$, $A_{42} = 2BCD(L_f - L_r)/I_z$, $A_{43} = -2BCD(L_f - L_r)/I_zRn$, $A_{44} = -2BCD(L_f^2 + L_r^2)/I_zRn$, $A_{55} = -B_m/J_m$, $A_{56} = K_t/J_m$, $A_{65} = -K_e/L_a$, and $A_{66} = -R_a/L_a$. In addition

$$A' = \begin{bmatrix} 0 & 0 & 0 & 0 & 0 & 0 \\ 0 & 0 & 0 & 0 & 0 & 0 \\ A'_{31} & 0 & A'_{33} & 0 & 0 & 0 \\ A'_{41} & 0 & A'_{43} & 0 & 0 & 0 \\ 0 & 0 & 0 & 0 & 0 & 0 \\ 0 & 0 & 0 & 0 & 0 & 0 \end{bmatrix}$$

where $A'_{31} = -2BCDK/m$, $A'_{33} = -2BCDKL/mRn$, $A'_{41} = -2BCDKL_f/I_z$, and $A'_{43} = -2BCDKLL_f/I_zRn$.

An ATDFC can be chosen as

$$u(t) = \widetilde{K}(t)\,[x(t) - x(t - T_c)] \tag{31}$$

where T_c denotes the controller delay time, and $\widetilde{K}(t)$ is the feedback gain matrix. This gain matrix can be tuned by an adaptive law, as given by

$$\widetilde{K}(t) = -\eta \int_0^t x^T(t) PB\,(x(t) - x(t - T_c))\,dt \tag{32}$$

where η is a positive constant, P is a positive definite and symmetric constant matrix, and B is a vector. Thus, the controlled system can be obtained as follows:

$$\dot{x}(t) = Ax(t) + A'x(t - T_r) + B\widetilde{K}(t)\,[x(t) - x(t - T_c)]\,. \tag{33}$$

To practically implement the ATDFC method, an easily measurable electrical parameter of the PMDC motor, namely the armature current I_a, is chosen as the feedback control parameter. Then, the whole control system can readily be implemented by a pulsewidth-modulated (PWM) dc-dc converter, as shown in Fig. 5, in which V_c is the control signal resulting from the difference between V_{in} and the ATDFC output, namely the

reference V_{in}^*, and the PWM pulse is generated by comparing V_c and the instantaneous sawtooth signal V_{st}.

The key to the ATDFC method is to determine proper values of the control matrix B, the positive value η, the positive definite symmetric matrix P, and T_c. First, the positive value η is chosen as 1.325. Second, since the I_a is chosen as the only feedback control signal, the control matrix B and the positive definite symmetric matrix P can be chosen as

$$B = \begin{bmatrix} 0 \\ 0 \\ 0 \\ 0 \\ 0 \\ 1 \end{bmatrix} \quad \text{and} \quad P = \begin{bmatrix} 1 & 0 & 0 & 0 & 0 & 0 \\ 0 & 1 & 0 & 0 & 0 & 0 \\ 0 & 0 & 1 & 0 & 0 & 0 \\ 0 & 0 & 0 & 1 & 0 & 0 \\ 0 & 0 & 0 & 0 & 1 & 0 \\ 0 & 0 & 0 & 0 & 0 & 5.3 \end{bmatrix}.$$

Finally, the T_c can be determined by using the gradient-descent approach, which is summarized by the following three steps. Relevant derivations and detailed discussions can be found in [22].

Step 1) Define a performance index as

$$J = \frac{1}{n}\sum_{i=1}^{n} \|x(t_0 + ih) - x(t_0 + ih - T_c)\|^2 \tag{34}$$

where h is the time step length, and n is the total number of time-series data. Then, the gradient can be derived as

$$\frac{\partial J}{\partial t} = \frac{2}{n}\sum_{i=1}^{n} [x(t_0 + ih) - x(t_0 + ih - T_c)]^T \dot{x}(t_0 + ih - T_c). \tag{35}$$

Step 2) Update the controller delay time T_c as

$$T_c(i+1) = T_c(i) - \beta \frac{\partial J}{\partial T_c(i)} \tag{36}$$

where β is a properly chosen positive parameter.

Step 3) Set a tolerance $\xi > 0$. If $J > \xi$, go to Step 2; otherwise, $\partial J/\partial t = 0$, and then the T_c becomes constant. In this paper, the controller delay time is chosen as $T_c = 7.325$ s.

V. Verification Results

By using MATLAB, numerical simulation is carried out. As shown in Fig. 6, chaos can be suppressed with respect to V_{in} equal to 107 V when the ATDFC takes effect after $t = 50$ s. It shows that both the amplitude and the frequency of ψ can be stabilized, confirming that the EV heading angle is prevented from the unstable oscillation by using the proposed ATDFC method. Thus, the safety performance of the EV steering system can be improved effectively.

In addition, Fig. 7(a) and (b) depicts the phase portraits of the ψ versus the velocity $\psi^{(1)}$. Fig. 7(a) shows a messy phase trajectory, which indicates that the EV heading angle oscillates at varying periods and displays a chaotic state. Meanwhile, Fig. 7(b) depicts the phase portrait after applying the ATDFC method at $t = 50$ s, which indicates that the EV steering system exhibits the stable periodic oscillation. Thus, it verifies that the proposed control method can suppress chaotic behaviors effectively.

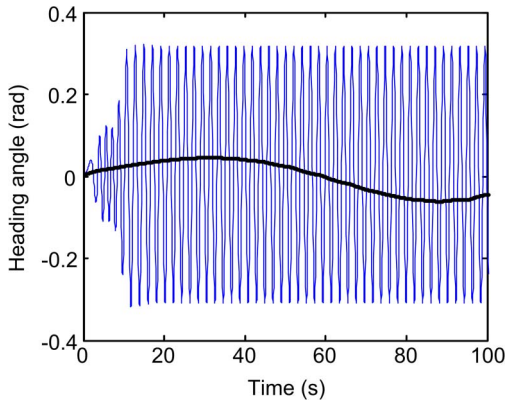

Fig. 8. Time responses of heading angle $\psi(T_r = 0.2$ s) using (thin line) conventional TDFC method and (thick line) ATDFC method.

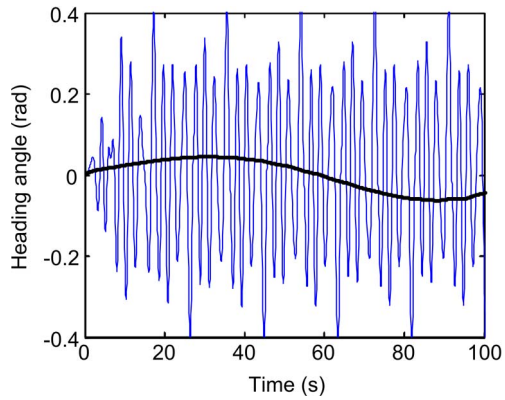

Fig. 9. Time responses of heading angle $\psi(T_r = 0.4$ s) using (thin line) conventional TDFC method and (thick line) ATDFC method.

To examine the robustness of the proposed control method, V_{in} is set as a constant value that is equal to 107 V. Then, $T_r = 0.2$ s is chosen to represent a fast response and $T_r = 0.4$ s to represent a slow response. The feedback gain of the conventional TDFC is chosen as $K = 0.12$. Fig. 8 shows that both the conventional TDFC and ATDFC methods can stabilize the EV steering system from chaos to the periodic oscillation. In terms of the control effect, however, the ATDFC method produces a much better performance than the conventional TDFC method. Additionally, as shown in Fig. 9, the conventional TDFC cannot suppress the chaos when the driver's response is slow ($T_r = 0.4$ s), whereas the ATDFC is still effective. Thus, the ATDFC method not only can offer a better control effect but also can improve the robustness of the EV steering system.

VI. Conclusion

In this paper, a new nonlinear dynamic model has been proposed to describe the steering system in EVs. As the engine of EVs, the PMDC motor is first introduced to analyze nonlinear dynamic characteristics of the EV steering system. In addition, this paper has taken into account the time delay resulting from the driver's response, which seriously affects the stability of the EV steering system. Moreover, the impact of

irregularities of the road surface is also considered as an external disturbances.

This paper provides the time responses, phase portraits, and power spectra to characterize dynamic behaviors of the EV steering system. First, the input voltage of the PMDC motor is chosen as the bifurcation parameter. The numerical simulation results have indicated that the EV steering system exhibits complex nonlinear dynamic behaviors with the increase in the PMDC motor input voltage, namely the periodic, multiperiodic, and chaotic motions. These unstable dynamic behaviors will deteriorate the safety performance of EVs. Additionally, the existence of chaos has been mathematically proven by calculating the largest Lyapunov exponent.

A new control method has been proposed and implemented to stabilize the EV steering system and thus improve the safety of EVs. By using the ATDFC method, the feedback gain can be tuned by an adaptive law to suppress the system parameter perturbation, such as the driver's reaction time. The simulation results have shown that dynamic behaviors of the EV steering system can be effectively stabilized from chaos to stable periodic oscillation.

It should be noted that the given EV steering system is based on the use of a relatively low-voltage low-power PMDC motor for propulsion; similar analysis can be extended to those high-end EV steering systems using a high-voltage high-power ac motor for propulsion but involving much more complicated coordinate transformation and field-oriented control.

APPENDIX

We consider a general continuous-time chaotic system with the time delay described by the following:

$$\dot{x}(t) = f\left(x(t)\right) + g\left(x(t-\tau)\right), \quad x(t_0) = x_0 \in R^n.$$

By using the Talyor expansion $(x = x_0)$, the linear differential equation can be obtained as

$$\dot{x}(t) = Ax(t) + A'x(t-\tau)$$

where $A = \partial f/\partial x(t)$, and $A' = \partial g/\partial x(t-\tau)$.

Suppose that the system is currently in the chaotic state and $\bar{x}(t)$ is the expected periodic solution as

$$\dot{\bar{x}}(t) = A\bar{x}(t) + A'\bar{x}(t-\tau).$$

Then, an ATDFC can be chosen as

$$u(t) = \widetilde{K}^T(t)\left(x(t) - x(t-\tau_C)\right)$$

where τ_C is the delay time, and $\widetilde{K}(t)$ denotes an adaptive tuned feedback gain that has a constant limit gain $\widetilde{K}^*$, as given by

$$\lim_{t\to\infty} \widetilde{K}(t) = \widetilde{K}^*.$$

Then, the controlled system can be obtained as

$$\dot{x}(t) = Ax(t) + A'x(t-\tau) + B\widetilde{K}^T(t)\left(x(t) - x(t-\tau_C)\right).$$

Consequently, the design problem is then to determine the feedback gain $\widetilde{K}(t)$ such that the controlled system orbit can track the target as follows:

$$\lim_{t\to\infty} \|x(t) - \bar{x}(t)\| = 0.$$

Taking $e = x(t) - \bar{x}(t)$ and $\Delta\widetilde{K}(t) = \widetilde{K}^* - \widetilde{K}(t)$, the corresponding error dynamic system can be obtained as

$$\begin{aligned}\dot{e}(t) &= \dot{x}(t) - \dot{\bar{x}}(t)\\ &= Ae(t) + A'e(t-\tau) + B\widetilde{K}^T(t)\\ &\quad\times\left(\bar{x}(t) + e(t) - \bar{x}(t-\tau_C) - e(t-\tau_C)\right).\end{aligned}$$

Without loss of generality, let $\bar{x}(t) = 0$. Thus, it yields

$$\dot{e}(t) = Ae(t) + A'e(t-\tau) + B\left(\widetilde{K}^* - \Delta\widetilde{K}(t)\right)^T\left(e(t) - e(t-\tau_C)\right).$$

Then, the control objective is to force $e(t) \to 0$ as $t \to \infty$.

Let us consider the following Lyapunov function candidate:

$$V(e, \Delta\widetilde{K}) = e^TPe + \int_{t-\tau}^{t} e^TUe\,dt + \int_{t-\tau_C}^{t} e^TVe\,dt + \frac{1}{\eta}\Delta\widetilde{K}^T\Delta\widetilde{K}$$

where P, U, and V are three positive definite matrices. Then, the derivative of Lyapunov function candidate is given by

$$\begin{aligned}\dot{V} &= \dot{e}^T(t)Pe(t) + e^T(t)P\dot{e}(t)\\ &\quad + e^T(t)Ue(t) - e^T(t-\tau)Ue(t-\tau) + e^T(t)Ve(t)\\ &\quad - e^T(t-\tau_C)Ve^T(t-\tau_C) - \frac{2}{\eta}\Delta\widetilde{K}^T(t)\dot{\widetilde{K}}(t)\\ &= -\left[U^{1/2}e(t-\tau) + U^{-1/2}A'^TPe(t)\right]^T\\ &\quad\times\left[U^{1/2}e(t-\tau) + U^{-1/2}A'^TPe(t)\right]\\ &\quad - \left[V^{1/2}e(t-\tau_C) + V^{-1/2}\widetilde{K}^*B^TPe(t)\right]^T\\ &\quad\times\left[V^{1/2}e(t-\tau_C) + V^{-1/2}\widetilde{K}^*B^TPe(t)\right] + e^T(t)\\ &\quad\times[A^TP + PA + U + V + PA'U^{-1}A'^TP\\ &\qquad + PB\widetilde{K}^{*T}V^{-1}\widetilde{K}^*B^TP + \widetilde{K}^*B^TP + PB\widetilde{K}^{*T}]e(t)\\ &\quad + 2\Delta\widetilde{K}^T\left[-1/\eta\dot{\widetilde{K}}(t) - e^T(t)PB\left(e(t) - e(t-\tau_C)\right)\right].\end{aligned}$$

Therefore, the adaptive feedback gain matrix $\widetilde{K}(t)$ can be chosen as

$$\widetilde{K}(t) = -\eta\int_0^t e^T(t)PB\left(e(t) - e(t-\tau_C)\right)dt.$$

Since P, U, and V are three positive definite and symmetric constant matrices, the Riccati polynomial matrix isbreak expressed as

$$\begin{aligned}A^TP + PA + PA'U^{-1}A'^TP + PB\widetilde{K}^{*T}V^{-1}\widetilde{K}^*B^TP\\ + \widetilde{K}^*B^TP + PB\widetilde{K}^{*T} + U + V\end{aligned}$$

which is either zero or seminegative definite ($= 0, \leq 0$ or < 0). Hence, the control objective can be achieved, i.e., $\|e(t)\| \to 0$ as $t \to \infty$, namely the system obits can track the expected state.

REFERENCES

[1] C. C. Chan and K. T. Chau, *Modern Electric Vehicle Technology*. London, U.K.: Oxford Univ. Press, 2001.

[2] K. T. Chau and C. C. Chan, "Emerging energy-efficient technologies for hybrid electric vehicles," *Proc. IEEE*, vol. 95, no. 4, pp. 821–835, Apr. 2007.

[3] J. Kasselmann and T. Keranen, "Adaptive steering," *Bendix Tech. J.*, vol. 2, pp. 26–35, May 1969.

[4] R. Fenton, G. Melocik, and K. Olson, "On the steering of automated vehicles: Theory and experiment," *IEEE Trans. Autom. Control*, vol. AC-21, no. 3, pp. 306–315, Jun. 1976.

[5] K. T. Chau and Z. Wang, *Chaos in Electric Drive Systems—Analysis, Control and Application*. Hoboken, NJ: Wiley-IEEE Press, 2011.

[6] J. H. Chen, K. T. Chau, and C. C. Chan, "Analysis of chaos in current-mode controlled DC drive systems," *IEEE Trans. Ind. Electron.*, vol. 47, no. 1, pp. 67–76, Feb. 2000.

[7] J. H. Chen, K. T. Chau, S. M. Siu, and C. C. Chan, "Experimental stabilization of chaos in a voltage-mode DC drive system," *IEEE Trans. Circuits Syst. I, Fundam. Theory Appl.*, vol. 47, no. 7, pp. 1093–1095, Jul. 2000.

[8] L. Dai and Q. Han, "Stability and Hopf bifurcation of a nonlinear model for a four-wheel-steering vehicle system," *Commun. Nonlin. Sci. Numer. Simul.*, vol. 9, no. 3, pp. 331–341, Jun. 2004.

[9] E. Ono, S. Hosoe, H. D. Tuan, and S. Doi, "Bifurcation in vehicle dynamics and robust front wheel steering control," *IEEE Trans. Control Syst. Technol.*, vol. 6, no. 3, pp. 412–420, May 1998.

[10] J. Ackermann, J. Guldner, W. Sienel, R. Steinhauser, and V. I. Utkin, "Linear and nonlinear controller design for robust automatic steering," *IEEE Trans. Control Syst. Technol.*, vol. 3, no. 1, pp. 132–143, Mar. 1995.

[11] B. A. Guvenc, L. Guvenc, and S. Karaman, "Robust yaw stability controller design and hardware-in-the-loop testing for a road vehicle," *IEEE Trans. Veh. Technol.*, vol. 58, no. 2, pp. 555–571, Feb. 2009.

[12] L. Cai, A. B. Rad, and W. Chan, "A genetic fuzzy controller for vehicle automatic steering control," *IEEE Trans. Veh. Technol.*, vol. 56, no. 2, pp. 529–543, Mar. 2007.

[13] A. E. Cetin, M. A. Adli, D. E. Barkana, and H. Kucuk, "Implementation and development of an adaptive steering-control system," *IEEE Trans. Veh. Technol.*, vol. 59, no. 1, pp. 75–83, Jan. 2010.

[14] P. Yih and J. C. Gerdes, "Modification of vehicle handling characteristics via steer-by-wire," *IEEE Trans. Control Syst. Technol.*, vol. 13, no. 6, pp. 965–976, Nov. 2005.

[15] P. Setlur, J. R. Wagner, D. M. Dawson, and D. Braganza, "A trajectory tracking steer-by-wire control system for ground vehicles," *IEEE Trans. Veh. Technol.*, vol. 55, no. 1, pp. 76–85, Jan. 2006.

[16] H. B. Pacejka and E. Bakker, "The magic formula tyre model," in *Proc. 1st Int. Colloquium Tyre Models Veh. Dyn. Anal.*, Delft, The Netherlands, Oct. 1992, pp. 1–18.

[17] T. Legouis, A. Laneville, P. Bourassa, and G. Payre, "Characterization of dynamic vehicle stability using two models of the human pilot behavior," *Veh. Syst. Dyn.*, vol. 15, no. 1, pp. 1–18, Jan. 1986.

[18] Z. Liu, G. Payre, and P. Bourassa, "Stability and oscillations in a time-delayed vehicle system with driver control," *Nonl. Dyn.*, vol. 35, no. 2, pp. 159–173, Jan. 2004.

[19] I. Shimada and T. Nagashima, "A numerical approach to ergodic problem of dissipative dynamical systems," *Progr. Theor. Phys.*, vol. 61, no. 6, pp. 1605–1616, Jun. 1979.

[20] J. D. Farmer, "Chaotic attractors of an infinite-dimensional dynamical system," *Phys. D*, vol. 4, no. 3, pp. 366–393, Mar. 1982.

[21] K. Pyragas, "Continuous control of chaos by self-controlling feedback," *Phys. Lett. A*, vol. 170, no. 6, pp. 421–428, Nov. 1992.

[22] G. Chen and X. Yu, "On time-delayed feedback control of chaotic systems," *IEEE Trans. Circuits Syst. I, Fundam. Theory Appl.*, vol. 46, no. 6, pp. 767–772, Jun. 1999.

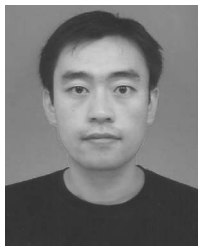

Zhen Zhang received the B.Eng. and M.Eng. degrees from Tianjin University, Tianjin, China, in 2004 and 2007, respectively. He is currently working toward the Ph.D. degree in electrical and electronic engineering with The University of Hong Kong, Pokfulam, Hong Kong.

His research interests include nonlinear analysis and control, electric vehicles, sustainable energy.

K. T. Chau (M'89–SM'04) received the B.Sc.(Eng.) (first-class honors), M.Phil., and Ph.D. degrees in electrical and electronic engineering from The University of Hong Kong, Pokfulam, Hong Kong, in 1988, 1991, and 1993, respectively.

He is currently a Professor with the Department of Electrical and Electronic Engineering and a Director with the International Research Center for Electric Vehicles, The University of Hong Kong. He is also a Chang Jiang Chair Professor with the Ministry of Education of China. He is the author of 400 refereed technical papers. He is also the author of two monographs: *Modern Electric Vehicle Technology* (Oxford Univ. Press, 2001) and *Chaos in Electric Drive Systems* (Wiley-IEEE Press, 2011). His teaching and research interests include electric vehicles, electric drives, and power electronics.

Dr. Chau is a Fellow of the Institution of Engineering and Technology and the Hong Kong Institution of Engineers.

Zheng Wang (S'05–M'09) received the B.Eng. and M.Eng. degrees from Southeast University, Nanjing, China, in 2000 and 2003, respectively, and the Ph.D. degree from The University of Hong Kong, Hong Kong, in 2008.

From 2008 to 2009, he was a Postdoctoral Fellow with Ryerson University, Toronto, ON, Canada. He is currently an Associate Professor with the School of Electrical Engineering, Southeast University, Nanjing. He is the author or coauthor of several technical papers and industrial reports in various areas. His research interests include power electronics, electric drives, and renewable energy techniques.